TITLE

Downregulation of *Let-7* miRNA promotes Tc17 differentiation and emphysema via de-repression of RORγt

AUTHORS

Phillip A. Erice[1,2], Xinyan Huang[2,6], Matthew J. Seasock[1,2], Matthew J. Robertson[3], Hui-Ying, Tung[4], Melissa A. Perez-Negron[2], Shivani L. Lotlikar[2], David B Corry[2,4,6], Farrah Kheradmand[4,5,6], Antony Rodriguez[2,6*]

[1]Immunology Graduate Program, Baylor College of Medicine, Houston, TX, 77030.

[2]Department of Medicine, Immunology & Allergy Rheumatology, Baylor College of Medicine Houston TX, 77030.

[3]Dan Duncan Comprehensive Cancer Center, Baylor College of Medicine Houston, TX, 77030.

[4]Department of Pathology and Immunology, Baylor College of Medicine Houston, TX, 77030.

[5]Department of Medicine, Section of Pulmonary and Critical Care, Baylor College of Medicine. Houston, TX, 77030.

[6]Center for Translational Research on Inflammatory Diseases, Michael E. Debakey, Baylor College of Medicine, Houston, TX, 77030.

[7]Current address, Department of Pulmonary and Critical Care Medicine, The First Affiliated Hospital of Sun Yat-sen University. Guangzhou, Guangdong Province, P.R. China

Author Correspondence: antony.rodriguez@bcm.edu

ABSTRACT

Environmental air irritants including nanosized carbon black (nCB) can drive systemic inflammation, promoting chronic obstructive pulmonary disease (COPD) and emphysema development. The *let-7* family of miRNAs is associated with IL-17-driven T cell inflammation, a canonical signature of lung inflammation. Recent evidence suggests the *let-7* family is

downregulated in patients with COPD, however, how they cause emphysema remains unclear. Here we show that overall expression of the *let-7* miRNA clusters, *let-7b/let-7c2* and *let-7a1/let-7f1/let-7d*, are reduced in the lungs and T cells of smokers with emphysema as well as in mice with cigarette smoke (CS)- or nCB-elicited emphysema. We demonstrate that loss of the *let-7b/let-7c2*-cluster in T cells predisposed mice to exaggerated CS- or nCB-elicited emphysema. Furthermore, ablation of the *let-7b/let-7c2-cluster* enhanced $CD8^+IL17a^+$ T cells (Tc17) formation in emphysema development in mice. Additionally, transgenic mice overexpressing *let-7* in T cells were resistant to Tc17 and $CD4^+$ T cells (Th17) development when exposed to nCB. Mechanistically, our findings reveal the master regulator of Tc17/Th17 differentiation, RAR-related orphan receptor gamma t (RORγt), as a direct target of *let-7* miRNA in T cells. Overall, our findings shed light on the *let-7*/RORγt axis as a braking and driving regulatory circuit in the generation of Tc17 cells and suggests a novel therapeutic approach for tempering the augmented IL-17-mediated response in emphysema.

INTRODUCTION

Chronic obstructive pulmonary disease (COPD) ranks as the third leading cause of mortality and is projected to account for over a billion deaths by the end of the twenty-first century (GBD Chronic Respiratory Disease Collaborators, 2020; *Findings from the Global Burden of Disease Study 2017*, 2019; Laniado-Laborín, 2009). Currently, there are no treatment options to reverse emphysema, the most clinically significant variant of COPD, which often is progressive despite smoking cessation (Bhavani et al., 2015; Anthonisen et al., 2002).

Inhalation of fine particulate matter smaller than 2.5 microns ($PM_{2.5}$) found in outdoor and indoor air pollution as well as tobacco smoke are risk factors for COPD development (Adeloye et al., 2022; Eisner et al., 2010; Hu et al., 2010). We have previously shown that nano-sized carbon

53 black (nCB), a noxious chemical constituent of $PM_{2.5}$ found in the lungs of smokers, activates
54 macrophages and dendritic cells orchestrating a pathogenic T cell-dependent inflammatory
55 response and emphysema in mice (Lu et al., 2015; You et al., 2015; Shan et al., 2009; C.-Y.
56 Chang et al., 2022).

57 Research over the last decade has pointed to the importance of dysfunctional
58 inflammatory T cells in human COPD lung tissue and animal models of emphysema (Grumelli et
59 al., 2004; Xu et al., 2012; Williams et al., 2021). Aberrant T cells are implicated in impaired host
60 defense, exaggerated inflammation, and loss of self-tolerance in COPD (Williams et al., 2021;
61 Chen et al., 2023; Hogg et al., 2004; Maeno et al., 2007; Xu et al., 2012). In this regard, we and
62 others have demonstrated the role and pathogenicity of activated IFN-γ and IL-17-secreting
63 subsets of $CD4^+$ and $CD8^+$ T lymphocytes including Th1, Th17, and Tc1 cells in clinical isolates
64 and in mice with COPD (Lu et al., 2015; You et al., 2015; Shan et al., 2009; S.-H. Lee et al., 2007;
65 Kheradmand et al., 2023). The IL-17-secreting Th17 cells are particularly important as they
66 promote the destruction of lung epithelium and recruitment of macrophages and neutrophils which
67 then release proteolytic enzymes such as matrix metalloproteinases (MMPs) involved in the
68 degradation of the lung structural matrix (Barnes, 2016; Hoenderdos & Condliffe, 2013). We
69 previously demonstrated that intranasal inhalation of nCB in mice is sufficient to induce
70 emphysema by stimulating T cell activation by dendritic cells and macrophages in mice. Moreover,
71 we found that genetic ablation of IL-17a can attenuate nCB- or cigarette smoke-induced alveolar
72 destruction and airway inflammation (Shan et al., 2012; You et al., 2015). More recently, IL-17A
73 and IL-17F secreting $CD8^+$ T cell (Tc17) subpopulation has been shown to play a critical role in
74 the pathogenesis of several autoimmune and inflammatory disorders (Globig et al., 2022; Huber
75 et al., 2013; Srenathan et al., 2016).

76 Both Th17 and Tc17, require the fate-deterministic transcription factor RAR-related orphan
77 receptor gamma t (RORγt, encoded by *Rorc*) for differentiation and production of IL-17a (Ivanov

78 et al., 2007). RORγt is the best-studied positive transcriptional regulator of IL-17a and IL-17f
79 (Ivanov et al., 2006). In accordance with the importance of IL-17a transcription, RORγt expression
80 has also been reported to be elevated in COPD patients and in mouse models of COPD (Chu et
81 al., 2011; Li et al., 2015). However, the upstream pathophysiologic mechanisms that contribute to
82 the induction of RORγt and differentiation of Tc17 cells in COPD have not been well elucidated.

83 We previously reported that *miR-22* inhibits HDAC4, promoting antigen-presenting cell
84 activation (APC) in the lungs and inducing Th17-mediated emphysema in response to CS or nCB
85 in mice (Lu et al., 2015). Additional miRNAs that control APC and/or T cell driven IL-17a^{+}
86 inflammation have been identified by others including the *let-7* miRNA family (Mai et al., 2012;
87 Angelou et al., 2020). MicroRNA expression-based studies have shown frequent downregulation
88 of members of the *let-7* miRNA family, including *let-7a, let-7b, let-7c*, *let-7d*, l*et-7e*, and *let-7f* in
89 human emphysematous lung tissue and in murine models of emphysema, but the mechanism(s)
90 of action remain ill-defined (Christenson et al., 2013; Pottelberge et al., 2011; Conickx et al., 2017;
91 Izzotti et al., 2009). *Let-7* microRNA genes are encoded across eight loci either as single genes
92 or as polycistronic clusters which have confounded their analysis *in vivo* (Rodriguez et al., 2004).
93 Previous studies used *Lin28b* transgenic overexpression in T cells to block the maturation and
94 processing of *the let-7* miRNA family. They showed an inhibitory role of *let-7* family in Th17-driven
95 response in murine model of experimental autoimmune encephalomyelitis (EAE) (Angelou et al.,
96 2020).

97 Here we found that *let-7* miRNA, notably the *let-7a3/let-7b* and *let-7a1/let-7f1/let-7d*
98 clusters, are suppressed in the T cells isolated from lungs of emphysema patients. Consistently,
99 the analogous murine *let-7b/let-7c2-* (*let-7bc2*) and *let-7a1/f1/d1-* (*let-7afd*) clusters were similarly
100 downregulated in pre-clinical emphysema models. We engineered mouse models with the
101 specific loss-of-function (LOF) mutations of the *let-7bc2* or *let-7afd* clusters (*let-7bc2*^{LOF}and *let-*
102 *7afd*^{LOF}, respectively) in T cells as well as an inducible *let-7g* gain-of-function (GOF) (*let-7*^{GOF})

103 model to determine the T cell-intrinsic role of *let-7* miRNA in emphysema pathogenesis. Deletion
104 of *let-7* miRNA in T cells worsened alveolar damage elicited by inhalation of CS or nCB, and
105 increased infiltration of immune cells in the airways, including IL-17-producing $CD8^+$ T (Tc17) cells.
106 Mechanistically, we found that *let-7* controls type 17 differentiation by directly targeting the
107 lineage-determining transcription factor, RORγt. In support of this conclusion, *let-7*^{GOF} mice were
108 resistant to nCB-mediated induction of RORγt and Tc17 responses. Thus, we show a previously
109 unappreciated role for *let-7* miRNA as a repressor of RORγt and a molecular brake to the IL-17a-
110 mediated T cell inflammation in emphysema.

111

112 **RESULTS**

113 **The *let-7bc2*- and *let-7afd-clusters* are downregulated in lungs and T cells in COPD.**

114 To explore the involvement of *let-7* in emphysema, we scrutinized the genomic locations and
115 transcriptional annotation of *let-7* members frequently downregulated in lung T cells isolated from
116 smoker's lungs as well as mouse models of emphysema. This combined approach showed close
117 linkage and high conservation of two *Let-7* clusters encoded from long intergenic non-coding RNA
118 (linc)-like precursors in humans and mice (Figure 1A). To shed light on whether these *Let-7*
119 clusters are downregulated in patients with COPD, we analyzed a published (GSE57148) lung
120 RNA-seq dataset obtained from COPD (N=98 and control (N=91) subjects (Kim et al., 2015). Our
121 analysis identified significant downregulation of the *Mirlet7ahg* and *Mirlet7bhg* gene cluster
122 transcripts in COPD compared to control subjects (Figure 1B). We carried out quantitative PCR
123 (qPCR) detection of *Let-7a,* which is encoded by both clusters, in lung tissue samples of smokers
124 with emphysema and non-emphysema controls, detecting significant downregulation of *Let-7a* in
125 emphysema samples relative to controls (Figure 1C). Because *Let-7* has been shown to
126 participate in IL-17^+ T cell responses (Angelou et al., 2020; Guan et al., 2013; Newcomb et al.,

127 2015), we next sought to determine if the expression pattern of *Mirlet7ahg* and *Mirlet7bhg*-derived
128 *Let-7* members are impaired in purified $CD4^+$ T cells from emphysematous lungs. In support of
129 our original hypothesis, the $CD4^+$ T cell expression of *Let-7a*, *Let-7b*, *Let-7d*, and *Let-7f* were all
130 inversely correlated with more severe emphysema distribution in the lungs as determined by CT
131 scan (Figure 1D).

132 Next, we elucidated *let-7a1/let-7f1/let-7d-* and *let-7b/let-7c2*-clusters expression (herein
133 referred to as *let-7afd* and *let-7bc2* respectively) in murine models of CS- or nCB-induced
134 emphysema respectively (Figure 1E). Paralleling our observations in human COPD and
135 emphysema, mice with CS- or nCB-induced emphysema exhibited reduced expression levels of
136 *pri-let7afd* and *pri-let7bc2* transcripts in the lung and from isolated lung $CD4^+$ and $CD8^+$ T cells
137 (Figure 1F,G,H). Collectively, our expression results indicate suppression of *let-7afd* and *let-7bc2-*
138 clusters in the lung and T cells in human and pre-clinical models of emphysema.

139

140 **Conditional deletion of the *let7bc2*-cluster in T cells enhances nCB- or CS-induced**
141 **emphysema.**

142 To investigate the *in vivo* requirement of the *let-7bc2-cluster* within T cells, we generated
143 conditional ready floxed mice (*let-7bc2*$^{flox/flox}$). We then crossed *let7-bc2*$^{flox/flox}$ mice with *CD4-Cre*
144 mice to generate *let-7bc2*$^{flox/flox}$; *CD4-Cre* LOF mice (denoted as *let-7bc2*^{LOF} mice hereafter)
145 (Figure 2A). This approach allowed us to conditionally delete the *let-7bc2* cluster in all T cells
146 derived from the $CD4^+CD8^+$ double-positive (DP) stage (P. Lee et al., 2001; Shi & Petrie, 2012).
147 We confirmed that *let-7bc2*^{LOF} mice exhibit robust conditional deletion of the *let-7bc2* cluster in
148 DP thymocytes and peripheral $CD8^+$ T and $CD4^+$ T cells (Figure 2B and data not shown). Our *let-*
149 *7bc2*^{LOF} adult mice were born at the expected Mendelian frequency and did not show any overt
150 histopathologic or inflammatory changes in lungs histopathology up to 1 year of age in comparison

151 to *let-7bc2*$^{f/f}$ control mice (Figure 1-figure supplement 1A,B,C,D and data not shown).
152 Furthermore, quantification of major immune populations and T cell subsets by flow cytometry in
153 *let-7bc2*^{LOF} were comparable to control mice under baseline conditions and with moderate aging
154 (Figure 1-figure supplement 1A,B,C,D).

155 We next exposed *let-7bc2*^{LOF} and *let-7bc2*$^{f/f}$ control mice to nCB or CS and examined the
156 lungs under the context of experimental emphysema. Histomorphometry measurements of mean
157 linear intercept (MLI) from hematoxylin and eosin (H&E)-stained sections revealed that the
158 enlargement of alveolar spaces sustained from either nCB- or CS-exposure was exaggerated in
159 *let-7bc2*^{LOF} mice relative to controls (Figure 2C-E). Chronic inflammation in emphysema is
160 characterized by the recruitment of macrophages and neutrophils to the lung tissue and airways
161 (Peleman et al., 1999; Senior & Anthonisen, 1998). Internally consistent with MLI measurements,
162 *let-7bc2*^{LOF} mice treated with nCB showed significantly increased airway infiltration of
163 macrophages and neutrophils in BAL fluid as compared to wild-type control animals (Figure 2F).
164 Concomitant with these findings, expression levels of *Mmp9* and *Mmp12*, which are secreted by
165 macrophages and neutrophils to degrade elastin and mediate alveolar damage, were elevated in
166 airways of *let-7bc2*^{LOF} mice exposed to CS versus controls (Figure 2G). Collectively, our data
167 suggests that the *let-7bc2*-cluster within T cells protects by dampening airway destruction and
168 inflammation because the absence of this cluster worsens the severity of experimental
169 emphysema in mice.

170

171 **The *let-7bc2* miRNA cluster negatively regulates T_C17 inflammation in emphysema.**

172 We sought to identify the T cell-intrinsic mechanisms that underlie the exaggerated
173 inflammation observed in emphysematous *let7bc2*^{LOF} mice. We focused on the IL-17-mediated T
174 cell response because it promotes neutrophil and macrophage recruitment in the lungs (Beringer

175 et al., 2016; Veldhoen, 2017; Shan et al., 2012). Previously, we established the induction of
176 $CD4^+IL17^+$ (Th17) cells along with $CD4^+IFNg^+$ (Th1) cells in mice with chronic nCB exposure (You
177 et al., 2015), however whether nCB similarly induces $CD8^+IL17a^+$ T cells (Tc17) or cytotoxic T
178 cells (Tc1) had not been studied. The flow cytometric profiling of lung T cells revealed enriched
179 proportions and counts of Tc1 and Tc17 cells in mice with nCB-emphysema and we confirmed the
180 induction of Th17 and Th1 cells (Figure 3A-B control PBS and control nCB). These findings
181 suggests that nCB elicits both the type 17 and type 1 T cell responses, consistent with CS and
182 elastase pre-clinical models of emphysema (Zhang et al., 2019).

183 We next interrogated the regulatory role of the *let-7bc2*-cluster in the type 17 and type 1
184 responses generated from exposure to nCB. Interestingly, *let-7bc2*^{LOF} mice showed increased
185 $CD8^+IL17a^+$ Tc17 cells relative to nCB control animals. In contrast, $CD8^+IFN^+$ and $GZMA^+$ Tc1
186 populations remained unperturbed with absence of the *let-7bc2* cluster, suggestive of a more
187 refined regulatory role on Tc17 differentiation (Figure 3A-B). There were no significant differences
188 in either Th1 or Th17 cells when comparing nCB-treated *let-7bc2*^{LOF} to wild-type controls,
189 indicating the *let-7bc2* cluster was dispensable for their generation (Figure 3C). Regulatory T cells
190 form a dynamic axis with Tc17/Th17 cells and act as a counterbalance to lung inflammation in
191 emphysema (Duan et al., 2016; Jin et al., 2014). Therefore, we examined whether Tc17 cell
192 alterations were driven by the *let-7bc2* cluster acting on regulatory T cells (Tregs). The *let-7bc2*^{LOF}
193 mice showed no significant difference in Tregs subset relative to controls in our model (Figure
194 3D). Together, our data support the notion that deletion of the *let-7bc2*-cluster is insufficient to
195 provoke Tc17 cell generation under homeostatic conditions. However, under the context of chronic
196 inflammation in emphysema, the loss of *let-7bc2*-cluster is intrinsic for the potentiation of T cells
197 towards Tc17 differentiation.

198 **The *let-7* family directly inhibits RORγt expression governing Tc17 differentiation in**
199 **emphysema.**

200 We utilized the TargetScan predictive algorithm to identify putative *let-7* microRNA targets
201 that are known to control the IL-17-mediated T cell response (Agarwal et al., 2015). This analysis
202 revealed that the 3'UTR region of *Rorc*, encoding RORγt, contains an evolutionarily conserved
203 and complementary motif for the *let-7* miRNA family (Figure 4A). Thus, we examined if *let7bc2*-
204 cluster loss in T cells would stimulate and enhance RORγt. Initially, we carried out flow cytometric
205 quantification for RORγt in thymocyte, splenic, and lung T cells of naïve control and *let7bc2*^{LOF}
206 mice up to 6-months of age. Our interrogation of RORγt mean fluorescent intensity (MFI) by flow
207 cytometry showed induction of RORγt in single-positive CD8^{+} and CD4^{+} thymocytes, as well as
208 peripheral splenic CD8^{+} and CD4^{+} T cells (Figure 4B). However, RORγt levels appeared
209 unchanged in purified lung CD8^{+} T cells and CD4^{+} T cells of naive *let-7bc2*^{LOF} mice, alluding to a
210 compensatory effect in homeostatic lung T cells (Figure 4B). Since we and others have shown
211 that miRNAs are frequently associated with stress-dependent phenotypes, we posited that
212 emphysematous *let-7bc2*^{LOF} T cells are poised towards induction of RORγt and production of
213 IL17^{+} subsets after challenge with nCB. Indeed, nCB-emphysematous *let-7bc*^{LOF} mice exhibited
214 enhanced RORγt protein levels in both CD8^{+} and CD4^{+} T cells relative to control mice with
215 emphysema (Figure 4C).

216 Because we had found that the *let-7afd*-cluster is downregulated in T cells isolated from
217 COPD lungs in human and mice, and that the *let-7* family operates with some functional
218 redundancy, we generated mice with conditional deletion of the *let7afd*-cluster in T cells (*let-7afd*$^{f/f}$*;*
219 *CD4-Cre*). The *let-7afd*$^{f/f}$*; CD4-Cre* (*let7afd*^{LOF}) mice aged up to 6-months did not exhibit lung
220 histopathology nor inflammatory changes (data not shown). Of particular interest, ablation of the
221 *let-7afd*-cluster enhanced levels of RORγt in thymic and peripheral T cells of mice (Figure 4D).
222 Overall, this indicates that independent *let-7* clusters restrain RORγt expression levels from
223 thymic development to peripheral T cells under homeostatic conditions. Next, we determined
224 whether loss of *let-7afd*-cluster in T cells likewise sensitizes mice towards induction of RORγt in

225 nCB-emphysema. Intranasal administration of nCB provoked increased RORγt expression in lung
226 T cells of *let-7afd*^{LOF} mice as compared to *let-7afd*$^{f/f}$ control mice (Figure 4E), supporting
227 overlapping functionality between the *let-7bc2* and *let-7afd*-clusters in repression of RORγt within
228 T cells.

229 To confirm that the *let-7* family negatively regulates Tc17 cell differentiation, at least in part,
230 cell autonomously in CD8$^+$ T cells, we purified naïve CD8$^+$ T cells from *let-7bc2*^{LOF} and control
231 mice spleens and cultured these cells *in vitro* in the presence of Tc17 polarizing (TGFβ, IL-6, anti-
232 IFNγ, IL-23, and IL-1β) or Tc1 polarizing (IL-2) conditions (Flores-Santibáñez et al., 2018). Our
233 flow cytometric analysis confirmed the enhanced commitment of *let-7*-cluster deficient CD8$^+$ T
234 cells towards Tc17 cells and IL-17a$^+$ production relative to control CD8$^+$ T cells (Figure 5A-B).
235 Moreover, enhanced Tc17 cell differentiation mirrored the increased IL-17a detected in the
236 supernatant from *in vitro* polarized cells as quantified by ELISA (Figure 5C). Parallel assessment
237 of Tc1 differentiation did not detect a difference in CD8$^+$IFNγ$^+$ cells (Figure 5A and Figure 5D).
238 Altogether, these data recapitulated our *in vivo* findings that the *let-7bc2* cluster negatively
239 regulates Tc17 response but is dispensable in Tc1 cells. Finally, to determine whether Tc17
240 differentiation is likewise controlled by the *let-7afd* cluster, we cultured naive CD8$^+$ splenocytes
241 from *let-7afd*^{LOF} and controls under Tc17 conditions. As we had observed with *let-7bc2*^{LOF},
242 absence of the *let-7afd* cluster in T cells further enhanced differentiation towards Tc17 cells as
243 quantified by flow cytometry and ELISA (Figure 5E-F).

244 Next, we focused on *Rorc* as a potential direct target of *let-7*, which could mechanistically
245 mediate enhanced Tc17 differentiation in *let7bc2*^{LOF} mice. Towards this objective, tested whether
246 *let-7bc2*^{LOF} naïve CD8$^+$ T cells show elevated RORγt expression under either Tc0 or Tc17
247 differentiation conditions. In agreement with enhanced Tc17 differentiation, RORγt expression
248 was differentially and significantly upregulated under both Tc0 and Tc17 differentiation conditions
249 in *let-7bc2*^{LOF} cells relative to controls (Figure 5G). To determine whether *let-7* directly represses

250 *Rorc* mRNA levels we cloned the 3'UTR of *Rorc* into luciferase constructs. These reporter assays
251 with *let-7b* expressing cells independently confirmed that *let-7b* represses *Rorc* (Figure 5H, left).
252 Furthermore, deletion of the putative *let-7* binding sequence (Figure 4A) abrogated repression
253 by *let-7b* (Figure 5H, right), thus confirming *Rorc* as a functional target of *let-7* miRNA. Overall,
254 these *in vitro* experiments readily recapitulated an upstream regulatory role for *let-7* in Tc17
255 differentiation, mediated in part, via direct suppression of RORγt.

256

257 **Enforced expression of *let-7* tempers RORγt T cell expression levels in experimental**
258 **emphysema**.

259 To explore a potential protective role of *let-7* miRNA in experimentally induced
260 emphysema, we generated mice which allowed for selective induction of *let-7* activity in T cells
261 using the published *rtTA-iLet7* mice (Zhu et al., 2011; Belteki et al., 2005). We bred the *rtTA-iLet7*
262 mice to *CD4-Cre* (here in referred to as *let-7*^{GOF}) to allow Cre-loxP/doxycycline dependent *let-7g*
263 overexpression in thymic DP-derived T cells (Figure 6A). Steady-state *let-7*^{GOF} and control (*rtTA-*
264 *iLet7*) mice were examined for compromised RORγt protein levels within thymocytes and
265 peripheral T cells. Providing further evidence of *let-7*-dependent regulation of *Rorc*, protein levels
266 of RORγt were suppressed in CD8^{+} and CD4^{+} T cells of *let-7*^{GOF} mice relative to controls (Figure
267 6B). To determine whether enforced expression of *let-7* offered protection from experimental
268 emphysema, *let-7*^{GOF} and control mice were treated with nCB and then examined for changes in
269 lung pathology and T cell type 17 responses. The *let-7*^{GOF} mice did not exhibit any signs of lung
270 inflammation or pathologic remodeling at baseline (Figure 6C-D and data not shown)
271 Histopathologic analysis revealed a comparable degree of lung alveolar distension via
272 morphometric measurements of MLI in nCB-treated *let-7*^{GOF} mice versus controls suggesting that
273 enforced *let-7* expression is insufficient to protect the lung from emphysema (Figure 6C-D). On
274 the other hand, evaluation of IL17^{+} response and RORγt levels in emphysematous lung T cells

275 demonstrated that, in contrast to control nCB-treated mice, *let-7*^{GOF} mice exhibited dampened
276 lung Tc17 and Th17 cell populations and were resistant to the induction of RORγt after nCB-
277 exposure (Figure 6F-6E). Taken together, our *let-7* LOF and GOF models demonstrate the
278 necessity and sufficiency of *let-7* miRNA to act as a molecular brake to the type 17 T cell response
279 through the direct regulation of RORγt, further our data suggests that nCB- or CS-mediated
280 suppression of this braking mechanism furthers inflammation and exacerbates emphysema
281 severity (Figure 6G).

282

283 **DISCUSSION**

284 MiRNA expression-based studies of COPD patients and mice exposed to CS have
285 reported downregulation of *let-7* miRNA expression in lung tissues (Conickx et al., 2017;
286 Christenson et al., 2013b; Schembri et al., 2009). We and others explored the consequence of
287 loss of *let-7* expression/activity with synthetic oligonucleotides, sponges, lentiviral antisense
288 knockdown, or via ectopic delivery of Lin28b (Polikepahad et al., 2010; Viswanathan et al., 2008;
289 Piskounova et al., 2011), but studies pinpointing the role of individual *let-7* clusters as potential
290 drivers of lung inflammation and COPD within T cells remained elusive. In the present study, we
291 established that the *let-7* miRNA family members encoded by the *let-7bc2*- and *let-7afd*-clusters
292 are downregulated in T cells from lungs of emphysema patients and emphysematous mice that
293 were exposed to CS or nCB. Correspondingly, we demonstrated that *in vivo* genetic ablation of
294 *let-7bc2-cluster* further sensitized mice to lung tissue destruction and emphysema upon treatment
295 with nCB or CS. Mechanistically, our studies suggests that *let-7* miRNA prevents the emergence
296 of $CD8^+$ T cell differentiation into Tc17 cells during emphysema in part, by directly silencing of
297 *Rorc*.

298 Tc17 cells are vital for defense against viral, fungal, and bacterial infections and they have
299 also been associated with inflammation in various human diseases such as multiple sclerosis,
300 inflammatory bowel disease, and cancer (Huber et al., 2013; Globig et al., 2022; Corgnac et al.,
301 2020). In accordance with the potential pathogenic role of Tc17 cells as drivers of COPD, several
302 studies detected increased cell numbers in airways and tissues of COPD patients as well as lungs
303 of smoke-exposed animal models (Chang et al., 2011; Zhou et al., 2020; Duan et al., 2013). Other
304 researchers also detected increased Tc17 subpopulations in tissues of COPD patients with
305 infectious microbial exacerbations. In our earlier work to define the adaptive T cell immune
306 responses in nCB induced COPD, we predominantly focused on the pathogenic role of Th17 cells,
307 but did not examine Tc17 cells (You et al., 2015). Here we expand upon our prior observations,
308 revealing that chronic exposure to nCB and elicitation of emphysema mice orchestrates the
309 emergence and accumulation of Tc17 cells which may act in parallel with Th17 cells to promote
310 tissue damage.

311 Although RORγt has been the subject of intense scrutiny and is subject to extensive
312 transcriptional and post-transcriptional regulatory control, to our knowledge this is the first
313 reported demonstration of miRNA-mediated gene silencing to RORγt. Our data also showed that
314 *in vivo* conditional genetic ablation of individual *let-7* clusters in T cells stimulates a rise in RORγt
315 protein expression in single-positive thymocytes and peripheral $CD8^+$ and $CD4^+$ T cells while
316 enforced *let-7* activity leads to partial repression of RORγt in T cells. Despite these alterations in
317 RORγt expression in our *let-7* T cell LOF and GOF mice, the mice did not exhibit spontaneous
318 gross phenotypes in thymus, spleens, or lungs at baseline. This may be due to the subtle and
319 modest expression thresholding of RORγt detected in mice and/or residual *let-7* expression in T
320 cells. On the other hand, and in agreement with our Tc17 and experimental emphysema data, we
321 observed enhanced RORγt expression and IL-$17a^+CD8^+$ T cells in lungs of *let-7* LOF mice after
322 treatment with nCB. We corroborated the importance of *let-7* activity in Tc17 differentiation of *ex*

323 *vivo* cultured CD8$^+$ T cells, as well as in the direct posttranscriptional control of RORγt, suggesting
324 that this defect, is in part, direct and cell autonomous. Interestingly, even though RORγt was
325 elevated in lung CD4$^+$ T cells to a similar extent as CD8$^+$ T cells, the enhanced IL17$^+$ responses
326 were limited to Tc17 subpopulation in the *let-7bc2*^{LOF} mice. Although, the *let-7afd*^{LOF} mice also
327 showed baseline induction of RORγt relative to controls in lung T cells the mice did not exhibit
328 changes in Tc17/Th17 subpopulations (data not shown). Nonetheless, it seems likely that under
329 different cellular contexts, the functions of *let-7*-clusters do not fully overlap in association with
330 differential thresholding of mRNA targets. Indeed, in B cells, the *let-7afd*-cluster is essential for an
331 antigen-specific antibody response, whereas the *let-7bc2*-cluster appears dispensable (Jiang et
332 al., 2018), iterating that differential physiological role of *let-7* clusters in the immune system and
333 validating an individual cluster approach in dissemination of mechanisms of *let*-7 in T cells. RORγt
334 is a defining transcription factor of the IL-17-secreting subset of immune cells, which also includes
335 γδ17 T cells, NKT17 and type 3 innate lymphoid cells, populations that contribute to COPD
336 pathology (Yanagisawa et al., 2017). A limitation of our study is that we did not examine whether
337 these populations were impacted by nCB-emphysema and/or in the context of *let-7* LOF.

338 Published studies revealed a protective role of *let-7* family against Th17-driven pathogenic
339 response in EAE attributed in part to direct regulation of *IL-1 receptor 1* and *IL-23 receptor*
340 (Angelou et al., 2020). Lending some support to these observations, we detected subtle transcript
341 level induction of *Il23r* in *let-7bc2*^{LOF} *in vitro* polarized Tc17 cells (data not shown). However, prior
342 publications on the role of *let-7* in T cells made use of *in vivo Lin28b* transgenic overexpression
343 in immune cells to block maturation and activity of the entire *let-7* miRNA family. Furthermore,
344 *Lin28b* was recently reported to influence transcriptome-wide ribosome occupancy and global
345 miRNA biogenesis (Tan et al., 2019) which could account for differences in scope of *let-7* targets
346 in those studies and ours. Nonetheless, further studies will be required to ascertain whether other

347 targets of *let-7* beyond RORγt synergistically potentiate the *in vivo* Tc17-response and
348 emphysema phenotype in *let7-bc2*^{LOF} T cells.

349 Tc17 cells play a major role in microbial infections, providing a potent anti-viral response
350 (Hamada et al., 2009; Yeh et al., 2010), while viral infection has been an established factor in
351 COPD exacerbations (Hewitt et al., 2016; Wedzicha, 2004). It will be interesting to determine
352 whether loss of *let-7bc2* or *let-7afd*-cluster activity in the T cell compartment contributes to COPD
353 disease susceptibility in the context of viral exposure. Our experiments with *let-7* GOF were
354 partially successful in limiting the emergence of Tc17 and Th17 in nCB-elicited emphysema but it
355 did not protect the lung from alveolar remodeling. Additional, studies will be required to ascertain
356 whether interventions that enhance *let-7* activity are successful in acute models of CS exposure
357 and COPD or in other chronic inflammation diseases associated with dysregulation of RORγt and
358 IL17^{+} injury.

359

360 **MATERIALS AND METHODS**

361 **Mice**

362 Conditional knockout-ready floxed *let-7bc2* and *let-7afd* mice were generated using CRISPR gene
363 editing in an isogenic C57BL/6 genetic background and were sequence verified for rigor. Mice
364 were PCR genotyped from ear samples with primers flanking loxP sites (Supplementary Table).
365 The *let-7bc2*$^{flox/flox}$; *CD4-cre* and *let-7afd*$^{flox/flox}$; *CD4-cre* mice were PCR genotyped. The *R26-*
366 *STOP-rtTA*; *Col1a1-tet0-let-7* (*rtTA-iLet7)* mice were obtained from JAX Jax Stocks 023912 and
367 05670 and then bred to *CD4-Cre* were PCR genotyped with established JAX primers. Control
368 *rtTA-iLet7* and the *let-7*^{GOF} mice were fed *ad libitum* with 200mg/kg of doxycycline-containing chow
369 (Bio-Serv S3888) at weaning age. Syngeneic littermates served as controls for all mouse
370 experiments. All mice were bred in the transgenic animal facility at Baylor College of Medicine. All
371 experimental protocols used in this study were approved by the Institutional Animal Care and Use

372 Committee of Baylor College of Medicine animal protocol (AN-7389) and followed the National
373 Research Council Guide for the Care and Use of Laboratory Animals.
374
375 **Human emphysema tissue samples and T cell isolation**
376 Lung tissues were obtained from a total of 28 non-atopic current or former smokers with significant
377 (>20 pack-years, one pack-year equals to smoking one pack of cigarettes per day each year)
378 history of smoking who were recruited into studies from the chest or surgical clinics at Michael E.
379 DeBakey Houston Veterans Affairs Medical Center hospitals (Shan et al., 2009). Human lung
380 single T cells were prepared from surgical resection and lungs in patients as previously described
381 by selection with biotin-labeled antibodies by autoMACs (Miltenyi Biotec) (Yuan et al., 2020;
382 Grumelli et al., 2004). Studies were approved by the Institutional Review Board at Baylor College
383 of Medicine and informed consent was obtained from all patients. Emphysema and non-
384 emphysema control patients were diagnosed from CT scans according to the criteria
385 recommended by the National Institutes of Health–World Health Organization workshop summary
386 (Pauwels et al., 2001).
387
388 **Human lung transcriptome data**
389 A publicly available RNA-seq dataset from a Korean cohort GSE57148 was selected for the
390 analysis (Kim et al., 2015). The raw FASTQ files of paired end reads representing the
391 transcriptome of control and cases were retrieved from the GEO database at the National Centre
392 for Biological Information (NCBI) through accession number GSE57148 and analyzed with R
393 package for differential expression.
394
395 **Cigarette smoke exposure model of pulmonary emphysema**
396 To promote emphysema, mice were exposed to cigarette smoke using our custom designed
397 whole-body inhalation system (Morales-Mantilla et al., 2020). In total, mice were exposed to four

398 cigarettes (Marlboro 100's; Philip Morris USA) per day, five days a week, for four months as
399 previously described (Morales-Mantilla et al., 2020, Shan et al., 2012).
400
401 **nCB exposure model of pulmonary emphysema**
402 Nano-sized particulate carbon black was prepared and administered as previously described (You
403 et al., 2015; Lu et al., 2015). Dried nCB nanoparticles were resuspended in sterile PBS to a
404 concentration of 10 mg/ml. Fifty µl of reconstituted nCB (0.5 mg) were intranasally delivered to
405 deeply anesthetized mice on a schedule of three times a week for four weeks (total delivered
406 dose of 6 mg). Lung histomorphometry and airway inflammation were assessed four weeks after
407 the final nCB challenge. For histomorphometric analysis, mice lungs were fixed with 10% neutral-
408 buffered formalin solution via a tracheal cannula at 25-cm H_2O pressure followed by paraffin
409 embedding and tissue sectioning and stained with hematoxylin and eosin. Mean linear intercept
410 (MLI) measurement of mouse lung morphometry were done as previously described (Shan et al.,
411 2014; Morales-Mantilla et al., 2020). Briefly, this was done in a blinded fashion to mice genotypes
412 from ten randomly selected fields of lung parenchyma sections. Paralleled lines were placed on
413 serial lung sections and MLI was calculated by multiplying the length and the number of lines per
414 field, divided by the number of intercepts (Morales-Mantilla et al., 2020).
415 BALF was collected by instilling and withdrawing 0.8 ml of sterile PBS twice through the
416 trachea. Total and differential cell counts in the BALF were determined with the standard
417 hemocytometer and HEMA3 staining (Biochemical Sciences Inc, Swedesboro, NJ) using 200 µL
418 of BALF for cytospin slide preparation (Morales-Mantilla et al., 2020; Lu et al., 2015).
419
420 **Cell isolation from murine lung tissue**
421 Mouse lung tissue were cut into 2-mm pieces and digested with collagenase type D (2 mg/ml;
422 Worthington) and deoxyribonuclease (DNase) I (0.04 mg/ml; Roche) for 1 hour in a 37°C
423 incubator. Single-cell suspensions from lung digest, spleen, and thymus were prepared by

424 mincing through 40-μm cell strainers then washing and resuspension in complete RPMI media.
425 Mouse lung and spleen single-cell suspensions were additionally overlaid on Lympholyte M cell
426 separation media (Cedarlane) as indicated in the manufacturer's protocol to purify lymphocytes.
427 For murine *let-7* expression studies, lung single-cell suspensions were labeled with anti-$CD4^+$ or
428 anti-$CD8^+$ magnetic beads and separated by autoMACS (Miltenyi Biotec), or $CD4^+CD8^+$ double
429 positive cells purified from thymus single-cell suspensions by flow-cytometric sorting on FACS
430 Aria (BD Biosciences).
431
432 ***In vitro* polarization of $CD8^+$ T cells**
433 $CD8^+$ naïve T cells were isolated from spleen using Mojosort Mouse CD8 Naïve T cell isolation
434 Kit (Biolegend) and adjusted to a concentration of $1.0x10^6$ cells/mL. Purified cells were activated
435 with plate-bound anti-CD3 (1.5μg/mL) and complete RPMI media containing anti-CD28
436 (1.5μg/mL) and β-mercaptoethanol (50nM) for Tc0 polarization, or further supplemented with Tc1
437 [IL-2 (10ng/mL)] or Tc17 [TGFβ (2ng/mL), IL-6 (20ng/mL), anti-IFNγ (10μg/mL), IL-23 (20ng/mL),
438 and IL-1β (5ng/mL)] polarization conditions for 72 hours (Flores-Santibáñez et al., 2018).
439
440 **ELISA**
441 Supernatant was collected from *in vitro* polarized murine $CD8^+$ T cells and centrifuged to remove
442 cellular debris. Cytokine levels of IL-17a and IFNγ were quantified from collected supernatant
443 using Mouse IL-17a Uncoated ELISA and Mouse IFN gamma Uncoated ELISA (Invitrogen) Kits,
444 respectively, per the manufacturer's instructions with colorimetric analysis by the Varioskan LUX
445 microplate reader (ThermoFisher).
446
447 **Flow cytometric analysis**
448 Cells used for *in vitro* or *in vivo* cytokine analysis were stimulated with PMA (20ng/mL; Sigma
449 Aldrich), Ionomycin (1μg/mL; Sigma Aldrich), and Brefeldin A (2μg/mL; Sigma Aldrich) for 4 hours

450 prior to flow staining (Lu et al., 2015). For intracellular staining, cells were fixed and permeabilized
451 using the Mouse FOXP3 Buffer Set (BD) per the manufacturer's protocol. The fluorophore-
452 conjugated antibodies used in this study were as follows: Live/Dead Fix Blue (Invitrogen), CD3
453 PerCPCy5.5 (Biolegend), TCRb PE/Cy7 (Biolegend), CD4 PB (Biolegend), CD4 AF700
454 (Biolegend), CD8 BV650 (Biolegend), CD25 BV421 (Biolegend), FOXP3 AF488 (Biolegend),
455 ROR gamma T PE (Invitrogen), TCF1 AF647 (Cell Signaling Technologies), TCF1 PE (Biolegend),
456 IFNγ AF647 (Biolegend), IL17a FITC (Biolegend), IL17a PE (ebioscience), PD1 BUV737 (BD),
457 TIM3 AF647 (R&D). Samples were analyzed using BD LSR II flow cytometer (BD Biosciences)
458 and FlowJo software (TreeStar),
459

460 **RNA Isolation and Quantitative RT-PCR**

461 RNA was isolated using miRNeasy (Qiagen) or RNeasy Mini Kit (Qiagen) in conjunction with the
462 RNase-Free DNase (Qiagen) according to the manufacturer's instructions. cDNA of miRNAs and
463 mRNAs were synthesized using TaqMan Advanced miRNA cDNA Synthesis Kit (ThermoFisher)
464 and High-Capacity cDNA Reverse Transcription Kit Real-Time PCR system (Applied Biosystems).
465 18S and snoRNA-202 were used to normalize mRNA and miRNA expression respectively.
466 Quantitative RT-PCR data were acquired on 7500 Real-Time PCR System or StepOne Real-Time
467 PCR System (Applied Biosystems) with the following TaqMan probes: *hsa-let-7a* [000377], *hsa-*
468 *let-7b* [000378], *hsa-let-7d* [002283], *hsa-let-7f* [000382], *pri-miR-let7a* [Mm03306744_pri], *pri-*
469 *miR-let7d* [Mm03306666_pri], *pri-miR-let7b* [Mm03306756_pri], *Mmp9* [Mm00442991], *Mmp12*
470 [Mm00500554].
471

472 **Luciferase reporter assays**

473 Genomic fragment containing the murine *Rorc* 3'UTR was cloned into psiCHECK2 luciferase
474 reporter plasmid (Promega). This construct was also used to generate the *let-7* 'seed' deletion
475 mutant derivative using the QuikChange Multi Site Mutagenesis Kit (catalog 200514-5,

476 Stratagene). 3T3 mouse embryonic fibroblasts (MEFs) were transfected using Oligofectamine
477 (Invitrogen) with 100 ng of psiCheck-2 plasmid containing wild-type or mutant 3'UTR, along with
478 the miRNA control or *let-7b* duplex (Dharmacon) at a final concentration of 6 nM (Gurha et al.,
479 2012). Reporter activity was detected with the Dual-Luciferase Reporter Assay System
480 (Promega).
481
482 **Statistical analysis**
483 Statistical analyses were performed using GraphPad Prism 10.0.1 software. Statistical
484 comparison between groups was performed using the unpaired Student's t-test, two-way analysis
485 of variance (ANOVA) with Tukey's or Sidak's correction, and Mann-Whitney Test when indicated.
486 A P-value less than 0.05 was considered statistically significant; ns indicates not significant.
487 Statistical significance values were set as *$p < 0.05$, **$p < 0.01$, ***$p < 0.001$, and ****$p < 0.0001$.
488 Data are presented as means ± SEM. P-value and sample sizes (n) are indicated in the figure
489 legends.
490
491 **COMPETING INTEREST STATEMENT**
492 The authors declare no competing interests.
493
494 **ACKNOWLEDGEMENTS**
495 We thank Jason Heaney and Denise Lanza at BCM Genetically Engineered Rodents Core
496 (funded in part by NIH P30 CA125123); Patricia Castro at Tissue Acquisition and Pathology Core
497 (funded in part by P30 CA125123); and Joel M. Sederstrom at the BCM and Cell Sorting Core
498 with funding from the CPRIT Core Facility Support Award (CPRIT-RP180672) and NIH
499 (CA125123 and RR024574). This work was supported by grants from the NHLBI (R01HL140398
500 to AR), the Gilson Longenbaugh Foundation (to A.R.), and NIEHS (T32 ES027801 to PE).
501

502 **AUTHOR CONTRIBUTIONS**

503 P.E., X.H., D.B.C, F.K., and A.R. conceptualized experiments and interpreted results. P.E., X.H.,
504 M.J.S., H.T., M.A.P., and S.L.L. acquired the data, M.J.R. provided bioinformatics analyses. P.E.
505 and A.R. wrote the manuscript.

506

507 **REFERENCES**

508 Agarwal, V., Bell, G. W., Nam, J.-W., & Bartel, D. P. (2015). Predicting effective microRNA
509 target sites in mammalian mRNAs. *eLife*, *4*, e05005. https://doi.org/10.7554/eLife.05005

510 Angelou, C. C., Wells, A. C., Vijayaraghavan, J., Dougan, C. E., Lawlor, R., Iverson, E.,
511 Lazarevic, V., Kimura, M. Y., Peyton, S. R., Minter, L. M., Osborne, B. A.,
512 Pobezinskaya, E. L., & Pobezinsky, L. A. (2020). Differentiation of Pathogenic Th17
513 Cells Is Negatively Regulated by Let-7 MicroRNAs in a Mouse Model of Multiple
514 Sclerosis. *Frontiers in Immunology*, *10*, 3125. https://doi.org/10.3389/fimmu.2019.03125

515 Barnes, P. J. (2016). Inflammatory mechanisms in patients with chronic obstructive pulmonary
516 disease. *Journal of Allergy and Clinical Immunology*, *138*(1), 16–27.
517 https://doi.org/10.1016/j.jaci.2016.05.011

518 Beringer, A., Noack, M., & Miossec, P. (2016). IL-17 in Chronic Inflammation: From Discovery
519 to Targeting. *Trends in Molecular Medicine*, *22*(3), 230–241.
520 https://doi.org/10.1016/j.molmed.2016.01.001

521 Chang, Y., Nadigel, J., Boulais, N., Bourbeau, J., Maltais, F., Eidelman, D. H., & Hamid, Q.
522 (2011). CD8 positive T cells express IL-17 in patients with chronic obstructive
523 pulmonary disease. *Respiratory Research*, *12*(1), 43. https://doi.org/10.1186/1465-9921-
524 12-43

525 Christenson, S. A., Brandsma, C.-A., Campbell, J. D., Knight, D. A., Pechkovsky, D. V., Hogg,
526 J. C., Timens, W., Postma, D. S., Lenburg, M., & Spira, A. (2013a). miR-638 regulates
527 gene expression networks associated with emphysematous lung destruction. *Genome*
528 *Medicine*, *5*(12), 114. https://doi.org/10.1186/gm519
529 Christenson, S. A., Brandsma, C.-A., Campbell, J. D., Knight, D. A., Pechkovsky, D. V., Hogg,
530 J. C., Timens, W., Postma, D. S., Lenburg, M., & Spira, A. (2013b). miR-638 regulates
531 gene expression networks associated with emphysematous lung destruction. *Genome*
532 *Medicine*, *5*(12), 114. https://doi.org/10.1186/gm519
533 Chu, S., Zhong, X., Zhang, J., Lao, Q., He, Z., & Bai, J. (2011). The expression of Foxp3 and
534 ROR gamma t in lung tissues from normal smokers and chronic obstructive pulmonary
535 disease patients. *International Immunopharmacology*, *11*(11), 1780–1788.
536 https://doi.org/10.1016/j.intimp.2011.06.010
537 Conickx, G., Avila Cobos, F., van den Berge, M., Faiz, A., Timens, W., Hiemstra, P. S., Joos, G.
538 F., Brusselle, G. G., Mestdagh, P., & Bracke, K. R. (2017). microRNA profiling in lung
539 tissue and bronchoalveolar lavage of cigarette smoke-exposed mice and in COPD
540 patients: A translational approach. *Scientific Reports*, *7*(1), Article 1.
541 https://doi.org/10.1038/s41598-017-13265-8
542 Corgnac, S., Malenica, I., Mezquita, L., Auclin, E., Voilin, E., Kacher, J., Halse, H., Grynszpan,
543 L., Signolle, N., Dayris, T., Leclerc, M., Droin, N., de Montpréville, V., Mercier, O.,
544 Validire, P., Scoazec, J.-Y., Massard, C., Chouaib, S., Planchard, D., … Mami-Chouaib,
545 F. (2020). CD103+CD8+ TRM Cells Accumulate in Tumors of Anti-PD-1-Responder
546 Lung Cancer Patients and Are Tumor-Reactive Lymphocytes Enriched with Tc17. *Cell*
547 *Reports Medicine*, *1*(7), 100127. https://doi.org/10.1016/j.xcrm.2020.100127

548 Duan, M.-C., Tang, H.-J., Zhong, X.-N., & Huang, Y. (2013). Persistence of Th17/Tc17 Cell
549 Expression upon Smoking Cessation in Mice with Cigarette Smoke-Induced Emphysema.
550 *Journal of Immunology Research*, *2013*, e350727. https://doi.org/10.1155/2013/350727
551 Duan, M.-C., Zhang, J.-Q., Liang, Y., Liu, G.-N., Xiao, J., Tang, H.-J., & Liang, Y. (2016).
552 Infiltration of IL-17-Producing T Cells and Treg Cells in a Mouse Model of Smoke-
553 Induced Emphysema. *Inflammation*, *39*(4), 1334–1344. https://doi.org/10.1007/s10753-
554 016-0365-8
555 *Findings from the Global Burden of Disease Study 2017*. (2019, January 4). Institute for Health
556 Metrics and Evaluation. https://www.healthdata.org/policy-report/findings-global-
557 burden-disease-study-2017
558 Globig, A.-M., Hipp, A. V., Otto-Mora, P., Heeg, M., Mayer, L. S., Ehl, S., Schwacha, H.,
559 Bewtra, M., Tomov, V., Thimme, R., Hasselblatt, P., & Bengsch, B. (2022). High-
560 dimensional profiling reveals Tc17 cell enrichment in active Crohn's disease and
561 identifies a potentially targetable signature. *Nature Communications*, *13*(1), Article 1.
562 https://doi.org/10.1038/s41467-022-31229-z
563 Grumelli, S., Corry, D. B., Song, L.-Z., Song, L., Green, L., Huh, J., Hacken, J., Espada, R., Bag,
564 R., Lewis, D. E., & Kheradmand, F. (2004). An Immune Basis for Lung Parenchymal
565 Destruction in Chronic Obstructive Pulmonary Disease and Emphysema. *PLOS*
566 *Medicine*, *1*(1), e8. https://doi.org/10.1371/journal.pmed.0010008
567 Guan, H., Fan, D., Mrelashvili, D., Hao, H., Singh, N. P., Singh, U. P., Nagarkatti, P. S., &
568 Nagarkatti, M. (2013). MicroRNA let-7e is associated with the pathogenesis of
569 experimental autoimmune encephalomyelitis. *European Journal of Immunology*, *43*(1),
570 104–114. https://doi.org/10.1002/eji.201242702

571 Hamada, H., Garcia-Hernandez, M. de la L., Reome, J. B., Misra, S. K., Strutt, T. M.,
572 McKinstry, K. K., Cooper, A. M., Swain, S. L., & Dutton, R. W. (2009). Tc17, a Unique
573 Subset of CD8 T Cells That Can Protect against Lethal Influenza Challenge1. *The*
574 *Journal of Immunology*, *182*(6), 3469–3481. https://doi.org/10.4049/jimmunol.0801814
575 Hewitt, R., Farne, H., Ritchie, A., Luke, E., Johnston, S. L., & Mallia, P. (2016). The role of
576 viral infections in exacerbations of chronic obstructive pulmonary disease and asthma.
577 *Therapeutic Advances in Respiratory Disease*, *10*(2), 158–174.
578 https://doi.org/10.1177/1753465815618113
579 Hoenderdos, K., & Condliffe, A. (2013). The Neutrophil in Chronic Obstructive Pulmonary
580 Disease. Too Little, Too Late or Too Much, Too Soon? *American Journal of Respiratory*
581 *Cell and Molecular Biology*, *48*(5), 531–539. https://doi.org/10.1165/rcmb.2012-0492TR
582 Huber, M., Heink, S., Pagenstecher, A., Reinhard, K., Ritter, J., Visekruna, A., Guralnik, A.,
583 Bollig, N., Jeltsch, K., Heinemann, C., Wittmann, E., Buch, T., Costa, O. P. da, Brüstle,
584 A., Brenner, D., Mak, T. W., Mittrücker, H.-W., Tackenberg, B., Kamradt, T., & Lohoff,
585 M. (2013). IL-17A secretion by $CD8^+$ T cells supports Th17-mediated autoimmune
586 encephalomyelitis. *The Journal of Clinical Investigation*, *123*(1), 247–260.
587 https://doi.org/10.1172/JCI63681
588 Ivanov, I. I., McKenzie, B. S., Zhou, L., Tadokoro, C. E., Lepelley, A., Lafaille, J. J., Cua, D. J.,
589 & Littman, D. R. (2006). The orphan nuclear receptor RORgammat directs the
590 differentiation program of proinflammatory IL-17+ T helper cells. *Cell*, *126*(6), 1121–
591 1133. https://doi.org/10.1016/j.cell.2006.07.035

592 Ivanov, I. I., Zhou, L., & Littman, D. R. (2007). Transcriptional Regulation of Th17 Cell
593 Differentiation. *Seminars in Immunology*, *19*(6), 409–417.
594 https://doi.org/10.1016/j.smim.2007.10.011
595 Izzotti, A., Calin, G. A., Arrigo, P., Steele, V. E., Croce, C. M., & De Flora, S. (2009).
596 Downregulation of microRNA expression in the lungs of rats exposed to cigarette smoke.
597 *The FASEB Journal*, *23*(3), 806–812. https://doi.org/10.1096/fj.08-121384
598 Jiang, S., Yan, W., Wang, S. E., & Baltimore, D. (2018). Let-7 Suppresses B Cell Activation
599 through Restricting the Availability of Necessary Nutrients. *Cell Metabolism*, *27*(2), 393-
600 403.e4. https://doi.org/10.1016/j.cmet.2017.12.007
601 Jin, Y., Wan, Y., Chen, G., Chen, L., Zhang, M.-Q., Deng, L., Zhang, J.-C., Xiong, X.-Z., & Xin,
602 J.-B. (2014). Treg/IL-17 Ratio and Treg Differentiation in Patients with COPD. *PLOS*
603 *ONE*, *9*(10), e111044. https://doi.org/10.1371/journal.pone.0111044
604 Kheradmand, F., Shan, M., Xu, C., & Corry, D. B. (2012). Autoimmunity in chronic obstructive
605 pulmonary disease: Clinical and experimental evidence. *Expert Review of Clinical*
606 *Immunology*, *8*(3), 285–292. https://doi.org/10.1586/eci.12.7
607 Kim, W. J., Lim, J. H., Lee, J. S., Lee, S.-D., Kim, J. H., & Oh, Y.-M. (2015). Comprehensive
608 Analysis of Transcriptome Sequencing Data in the Lung Tissues of COPD Subjects.
609 *International Journal of Genomics*, *2015*, 206937. https://doi.org/10.1155/2015/206937
610 Laniado-Laborín, R. (2009). Smoking and Chronic Obstructive Pulmonary Disease (COPD).
611 Parallel Epidemics of the 21st Century. *International Journal of Environmental Research*
612 *and Public Health*, *6*(1), Article 1. https://doi.org/10.3390/ijerph6010209
613 Lee, P. P., Fitzpatrick, D. R., Beard, C., Jessup, H. K., Lehar, S., Makar, K. W., Pérez-Melgosa,
614 M., Sweetser, M. T., Schlissel, M. S., Nguyen, S., Cherry, S. R., Tsai, J. H., Tucker, S.

615 M., Weaver, W. M., Kelso, A., Jaenisch, R., & Wilson, C. B. (2001). A Critical Role for
616 Dnmt1 and DNA Methylation in T Cell Development, Function, and Survival. *Immunity*,
617 *15*(5), 763–774. https://doi.org/10.1016/S1074-7613(01)00227-8
618 Lee, S.-H., Goswami, S., Grudo, A., Song, L.-Z., Bandi, V., Goodnight-White, S., Green, L.,
619 Hacken-Bitar, J., Huh, J., Bakaeen, F., Coxson, H. O., Cogswell, S., Storness-Bliss, C.,
620 Corry, D. B., & Kheradmand, F. (2007). Antielastin autoimmunity in tobacco smoking-
621 induced emphysema. *Nature Medicine*, *13*(5), 567–569. https://doi.org/10.1038/nm1583
622 Li, H., Liu, Q., Jiang, Y., Zhang, Y., Xiao, W., & Zhang, Y. (2015). Disruption of Th17/Treg
623 Balance in the Sputum of Patients With Chronic Obstructive Pulmonary Disease. *The*
624 *American Journal of the Medical Sciences*, *349*(5), 392–397.
625 https://doi.org/10.1097/MAJ.0000000000000447
626 Lu, W., You, R., Yuan, X., Yang, T., Samuel, E. L. G., Marcano, D. C., Sikkema, W. K. A.,
627 Tour, J. M., Rodriguez, A., Kheradmand, F., & Corry, D. B. (2015). MicroRNA-22
628 Inhibits Histone Deacetylase 4 to Promote T Helper-17 Cell-Dependent Emphysema.
629 *Nature Immunology*, *16*(11), 1185–1194. https://doi.org/10.1038/ni.3292
630 Mai, J., Virtue, A., Maley, E., Tran, T., Yin, Y., Meng, S., Pansuria, M., Jiang, X., Wang, H., &
631 Yang, X.-F. (2012). MicroRNAs and other mechanisms regulate interleukin-17 cytokines
632 and receptors. *Frontiers in Bioscience (Elite Edition)*, *4*, 1478–1495.
633 Morales-Mantilla, D. E., Huang, X., Erice, P., Porter, P., Zhang, Y., Figueroa, M., Chandra, J.,
634 King, K. Y., Kheradmand, F., & Rodríguez, A. (2020). Cigarette Smoke Exposure in
635 Mice using a Whole-Body Inhalation System. *JoVE (Journal of Visualized Experiments)*,
636 *164*, e61793. https://doi.org/10.3791/61793

637 Newcomb, D. C., Cephus, J. Y., Boswell, M. G., Fahrenholz, J. M., Langley, E. W., Feldman, A.
638 S., Zhou, W., Dulek, D. E., Goleniewska, K., Woodward, K. B., Sevin, C. M., Hamilton,
639 R. G., Kolls, J. K., & Peebles, R. S. (2015). Estrogen and progesterone decrease let-7f
640 microRNA expression and increase IL-23/IL-23 receptor signaling and IL-17A
641 production in patients with severe asthma. *Journal of Allergy and Clinical Immunology*,
642 *136*(4), 1025-1034.e11. https://doi.org/10.1016/j.jaci.2015.05.046
643 Pauwels, R. A., Buist, A. S., Calverley, P. M. A., Jenkins, C. R., & Hurd, S. S. (2001). Global
644 Strategy for the Diagnosis, Management, and Prevention of Chronic Obstructive
645 Pulmonary Disease. *American Journal of Respiratory and Critical Care Medicine*,
646 *163*(5), 1256–1276. https://doi.org/10.1164/ajrccm.163.5.2101039
647 Peleman, R. A., Rytila, P. H., Kips, J. C., Joos, G. F., & Pauwels, R. A. (1999). The cellular
648 composition of induced sputum in chronic obstructive pulmonary disease. *European*
649 *Respiratory Journal*, *13*(4), 839–843. https://doi.org/10.1034/j.1399-3003.1999.13d24.x
650 Pottelberge, G. R. V., Mestdagh, P., Bracke, K. R., Thas, O., Durme, Y. M. T. A. van, Joos, G.
651 F., Vandesompele, J., & Brusselle, G. G. (2011). MicroRNA Expression in Induced
652 Sputum of Smokers and Patients with Chronic Obstructive Pulmonary Disease. *American*
653 *Journal of Respiratory and Critical Care Medicine*, *183*(7), 898–906.
654 https://doi.org/10.1164/rccm.201002-0304OC
655 Prevalence and attributable health burden of chronic respiratory diseases, 1990–2017: A
656 systematic analysis for the Global Burden of Disease Study 2017. (2020). *The Lancet.*
657 *Respiratory Medicine*, *8*(6), 585–596. https://doi.org/10.1016/S2213-2600(20)30105-3

658 Rodriguez, A., Griffiths-Jones, S., Ashurst, J. L., & Bradley, A. (2004). Identification of
659 Mammalian microRNA Host Genes and Transcription Units. *Genome Research*, *14*(10a),
660 1902–1910. https://doi.org/10.1101/gr.2722704
661 Schembri, F., Sridhar, S., Perdomo, C., Gustafson, A. M., Zhang, X., Ergun, A., Lu, J., Liu, G.,
662 Zhang, X., Bowers, J., Vaziri, C., Ott, K., Sensinger, K., Collins, J. J., Brody, J. S., Getts,
663 R., Lenburg, M. E., & Spira, A. (2009). MicroRNAs as modulators of smoking-induced
664 gene expression changes in human airway epithelium. *Proceedings of the National*
665 *Academy of Sciences*, *106*(7), 2319–2324. https://doi.org/10.1073/pnas.0806383106
666 Senior, R. M., & Anthonisen, N. R. (1998). Chronic Obstructive Pulmonary Disease (COPD).
667 *American Journal of Respiratory and Critical Care Medicine*, *157*(4), S139–S147.
668 https://doi.org/10.1164/ajrccm.157.4.nhlbi-12
669 Shan, M., Cheng, H.-F., Song, L., Roberts, L., Green, L., Hacken-Bitar, J., Huh, J., Bakaeen, F.,
670 Coxson, H. O., Storness-Bliss, C., Ramchandani, M., Lee, S.-H., Corry, D. B., &
671 Kheradmand, F. (2009). Lung Myeloid Dendritic Cells Coordinately Induce TH1 and
672 TH17 Responses in Human Emphysema. *Science Translational Medicine*, *1*(4), 4ra10-
673 4ra10. https://doi.org/10.1126/scitranlsmed.3000154
674 Shan, M., You, R., Yuan, X., Frazier, M. V., Porter, P., Seryshev, A., Hong, J.-S., Song, L.,
675 Zhang, Y., Hilsenbeck, S., Whitehead, L., Zarinkamar, N., Perusich, S., Corry, D. B., &
676 Kheradmand, F. (2014). Agonistic induction of PPARγ reverses cigarette smoke–induced
677 emphysema. *The Journal of Clinical Investigation*, *124*(3), 1371–1381.
678 https://doi.org/10.1172/JCI70587
679 Shan, M., Yuan, X., Song, L., Roberts, L., Zarinkamar, N., Seryshev, A., Zhang, Y., Hilsenbeck,
680 S., Chang, S.-H., Dong, C., Corry, D. B., & Kheradmand, F. (2012). Cigarette Smoke

681 Induction of Osteopontin (SPP1) Mediates TH17 Inflammation in Human and
682 Experimental Emphysema. *Science Translational Medicine*, *4*(117), 117ra9-117ra9.
683 https://doi.org/10.1126/scitranslmed.3003041
684 Shi, J., & Petrie, H. T. (2012). Activation Kinetics and Off-Target Effects of Thymus-Initiated
685 Cre Transgenes. *PLoS ONE*, *7*(10), e46590. https://doi.org/10.1371/journal.pone.0046590
686 Veldhoen, M. (2017). Interleukin 17 is a chief orchestrator of immunity. *Nature Immunology*,
687 *18*(6), Article 6. https://doi.org/10.1038/ni.3742
688 Wedzicha, J. A. (2004). Role of Viruses in Exacerbations of Chronic Obstructive Pulmonary
689 Disease. *Proceedings of the American Thoracic Society*, *1*(2), 115–120.
690 https://doi.org/10.1513/pats.2306030
691 Williams, M., Todd, I., & Fairclough, L. C. (2021). The role of CD8 + T lymphocytes in chronic
692 obstructive pulmonary disease: A systematic review. *Inflammation Research*, *70*(1), 11–
693 18. https://doi.org/10.1007/s00011-020-01408-z
694 Xu, C., Hesselbacher, S., Tsai, C.-L., Shan, M., Spitz, M., Scheurer, M., Roberts, L., Perusich,
695 S., Zarinkamar, N., Coxson, H., Krowchuk, N., Corry, D., & Kheradmand, F. (2012).
696 Autoreactive T Cells in Human Smokers is Predictive of Clinical Outcome. *Frontiers in*
697 *Immunology*, *3*. https://www.frontiersin.org/articles/10.3389/fimmu.2012.00267
698 Yeh, N., Glosson, N. L., Wang, N., Guindon, L., McKinley, C., Hamada, H., Li, Q., Dutton, R.
699 W., Shrikant, P., Zhou, B., Brutkiewicz, R. R., Blum, J. S., & Kaplan, M. H. (2010).
700 Tc17 Cells Are Capable of Mediating Immunity to Vaccinia Virus by Acquisition of a
701 Cytotoxic Phenotype. *The Journal of Immunology*, *185*(4), 2089–2098.
702 https://doi.org/10.4049/jimmunol.1000818

703 You, R., Lu, W., Shan, M., Berlin, J. M., Samuel, E. L., Marcano, D. C., Sun, Z., Sikkema, W.
704 K., Yuan, X., Song, L., Hendrix, A. Y., Tour, J. M., Corry, D. B., & Kheradmand, F.
705 (2015). Nanoparticulate carbon black in cigarette smoke induces DNA cleavage and
706 Th17-mediated emphysema. *eLife*, *4*, e09623. https://doi.org/10.7554/eLife.09623
707 Zhang, H., Zhou, X., Chen, X., Lin, Y., Qiu, S., Zhao, Y., Tang, Q., Liang, Y., & Zhong, X.
708 (2019). Rapamycin attenuates Tc1 and Tc17 cell responses in cigarette smoke-induced
709 emphysema in mice. *Inflammation Research*, *68*(11), 957–968.
710 https://doi.org/10.1007/s00011-019-01278-0
711 Zhou, J.-S., Li, Z.-Y., Xu, X.-C., Zhao, Y., Wang, Y., Chen, H.-P., Zhang, M., Wu, Y.-F., Lai,
712 T.-W., Di, C.-H., Dong, L.-L., Liu, J., Xuan, N.-X., Zhu, C., Wu, Y.-P., Huang, H.-Q.,
713 Yan, F.-G., Hua, W., Wang, Y., … Shen, H.-H. (2020). Cigarette smoke-initiated
714 autoimmunity facilitates sensitisation to elastin-induced COPD-like pathologies in mice.
715 *European Respiratory Journal*, *56*(3). https://doi.org/10.1183/13993003.00404-2020
716 Zhu, H., Shyh-Chang, N., Segrè, A. V., Shinoda, G., Shah, S. P., Einhorn, W. S., Takeuchi, A.,
717 Engreitz, J. M., Hagan, J. P., Kharas, M. G., Urbach, A., Thornton, J. E., Triboulet, R.,
718 Gregory, R. I., Altshuler, D., & Daley, G. Q. (2011). The Lin28/let-7 Axis Regulates
719 Glucose Metabolism. *Cell*, *147*(1), 81–94. https://doi.org/10.1016/j.cell.2011.08.033

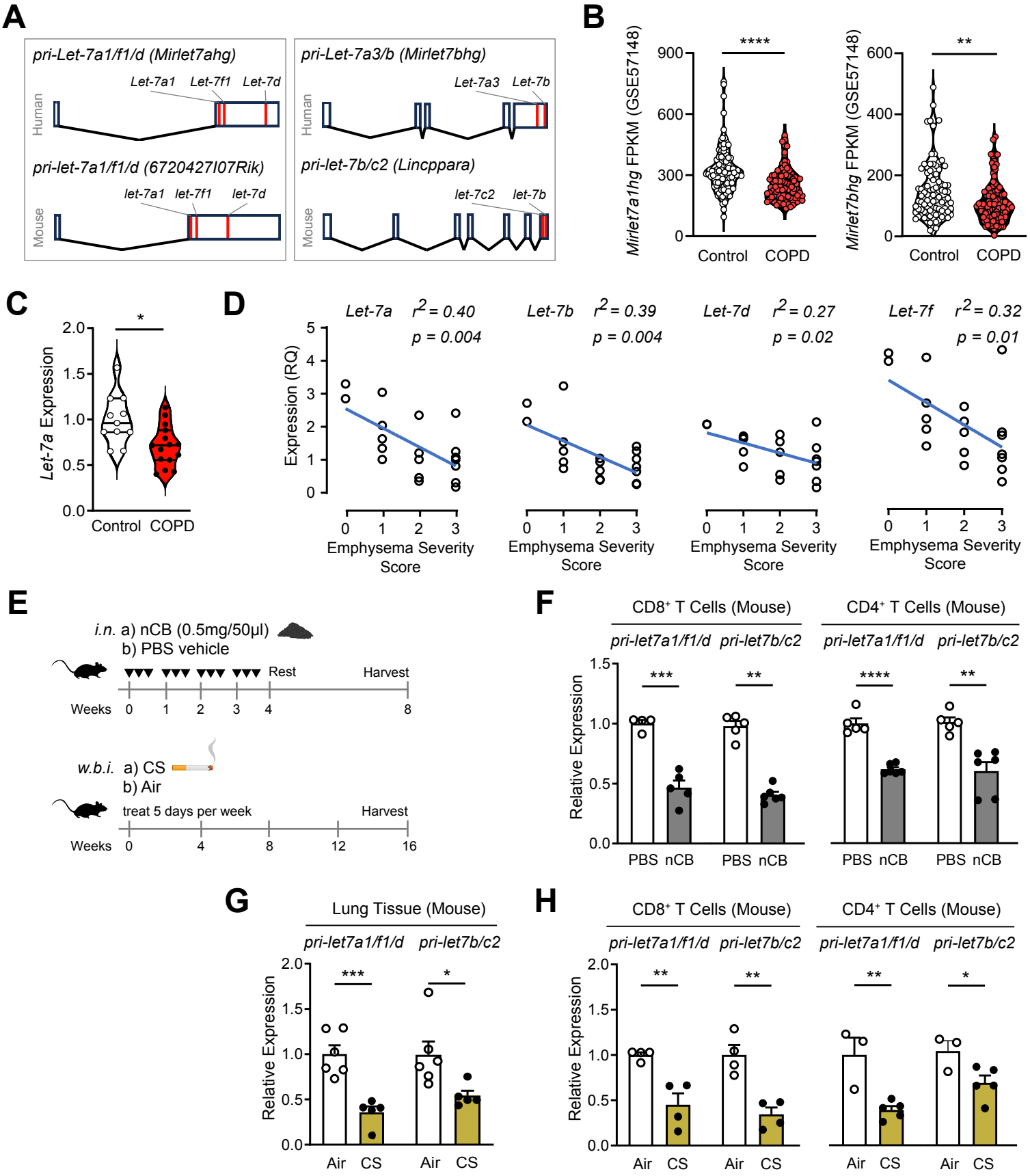

Figure 1. Repression of *Let-7* miRNA gene clusters in lung T cells from COPD patients and murine models of emphysema. (A) Schematic representation of the polycistronic transcripts for the *Let-7a1/Let-7f1/Let-7d-* and *Let-7b/Let-7a3*-clusters in humans and *let-7a1/let-7f1/let-7/d-* and l*et-7b/let-7c2*-clusters in mice. (B) *in silico* analysis of *Mirlet7a1hg* and *Mirlet7bhg* from the publicly available lung transcriptome dataset from RNA-seq of COPD and control patients (GEO: GSE57148). (C) Quantitative RT-PCR (qPCR) of mature *Hsa-Let-7a* from resected lung tissue of COPD (n=15) and control subjects (n=11). (D) qPCR and regression analysis of *Hsa-Let-7a, Hsa-Let-7b, Hsa-Let-7d, and Hsa-Let-7f* expression to emphysema severity score based on CT: 0=no, 1=upper lobes only, 2=upper/middle lobes, 3=extensive pan lobular emphysema (n=19). (E) Schematic diagram of experimental emphysema in mice induced by either intranasal (i.n.) instillation of nCB or exposure to CS by whole-body inhalation (w.b.i.). (F-H) qPCR analysis for *pri-let-7a1/f1/d* and *pri-let-7b/c2* from lung tissue or lung-derived CD8⁺ and CD4⁺ T cells of mice with emphysema elicited by (F) nCB- or (G-H) CS (n=3-6 per group). Data are representative of three independent experiments displayed as mean±SEM. Mann-Whitney (B,C) or Student's t-test (F,G,H). *p < 0.05, **p < 0.01, ***p <0.001, ****p<0.0001.

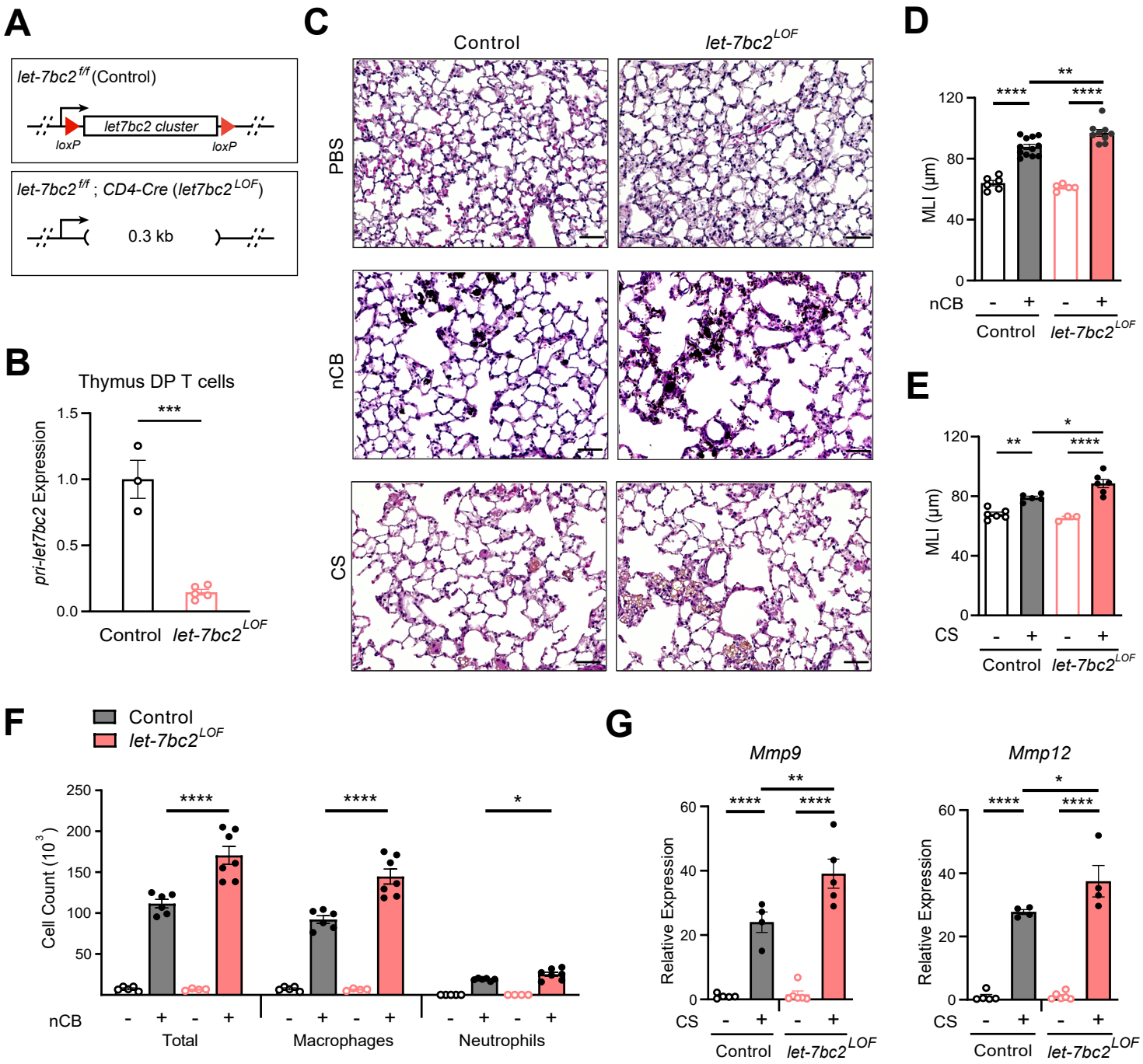

Figure 2. Deletion of the *let7bc2* cluster in T cells enhances nCB- or CS-triggered emphysema. (A) Schematic representation of CD4-Cre (*let-7bc2*^{LOF}) or *let-7bc2*$^{f/f}$ (Control) mice. (B) qPCR analysis of pri-miRNA transcript for *pri-let-7bc2* from flow-sorted live, TCRβ^{+}, CD4^{+}CD8^{+} double-positive (DP) thymocytes of control and *let-7bc2*^{LOF} mice (n=3-5 per group). (C-G) Control and *let-7bc2*^{LOF} mice were exposed to vehicle (PBS) or nCB for 4 weeks, or alternatively air or cigarette smoke by whole body inhalation of cigarette smoke (CS) for 16 weeks. (C) Representative H&E stained lung sections from PBS-, nCB-, or CS-exposed mice as indicated on each panel (x20 magnification; scale bars, 50µm). (D-E) Mean linear intercept (MLI) measurement of lung morphometry. (F) Total and differential cell counts from bronchoalveolar lavage (BAL) fluid from controls and nCB-emphysemic mice (n=4-7 per group). (G) *Mmp9* and *Mmp12* mRNA expression from BAL cells of air- and smoke-exposed control and *let-7bc2*^{LOF} mice (n=4-6 per group). Data are representative of at least three independent experiments displayed as mean±SEM using Student's t-test (B) or two-way ANOVA with *post-hoc* Tukey correction (D,E,F,G). *p < 0.05, **p < 0.01, ***p <0.001, ****p<0.0001.

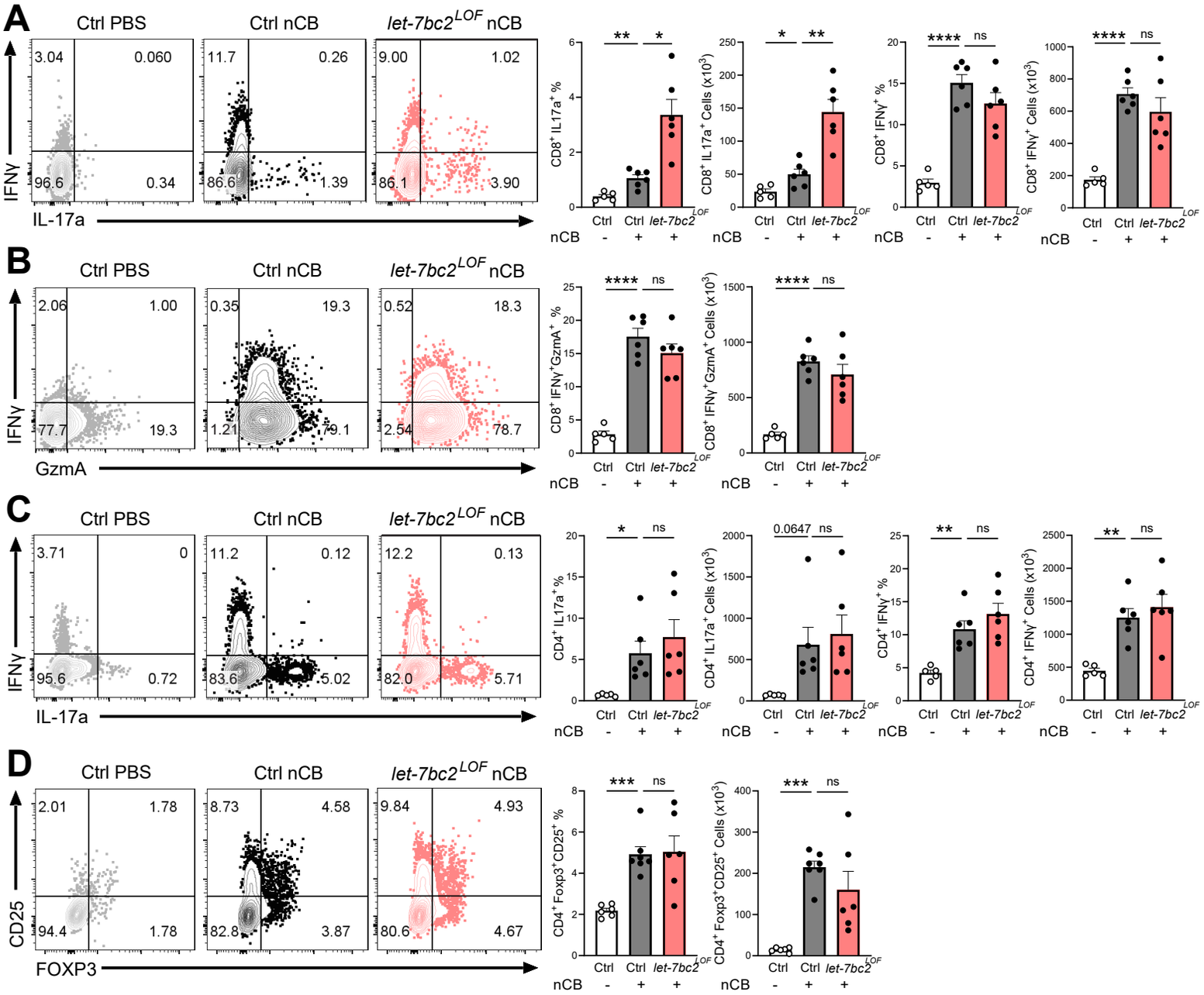

Figure 3. *In vivo* T cell ablation of the *let-7bc2*-cluster enhances Tc17 inflammatory response to nCB-emphysema. Representative flow plots with percentage and counts of live TCRβ⁺ (A) CD8⁺IL-17a⁺ and CD8⁺IFNγ⁺, (B) CD8⁺IFNγ⁺GzmA⁺, (C) CD4⁺IL-17a⁺ and CD4⁺IFNγ⁺, and (D) CD4⁺ Foxp3⁺CD25⁺ cells from the lungs of control PBS vehicle- (n=5-6), control nCB- (n=6), and *let-7bc2*^{LOF} nCB-exposed mice. Data are representa-tive of three independent experiments displayed as mean±SEM using ANOVA with *post-hoc* Sidak correction. *p < 0.05, **p < 0.01, ***p <0.001, ****p<0.0001.

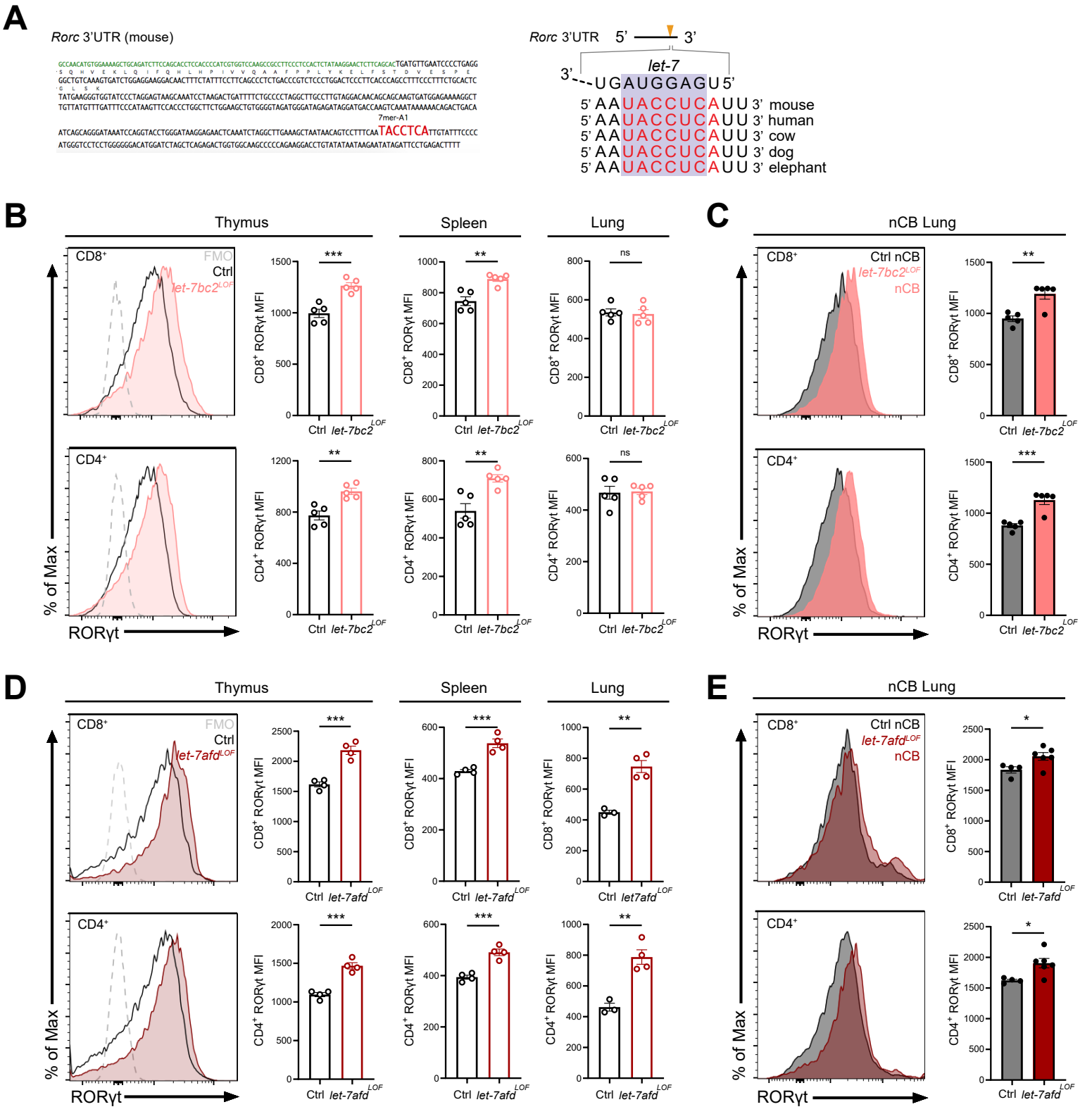

Figure 4. Deletion of either the *let7bc2*- or *let7afd*-cluster in T cells enhances RORγt expression *in vivo*. (A) Left: Schematic representation of the murine *Rorc* 3'UTR with *let-7* miRNA binding sites as identified by TargetScan. Right: Schematic of a conserved *let-7* miRNA target sequence in the 3'UTR of *Rorc*. (B-C) Flow analysis of RORγt expression by MFI quantification in live TCRβ⁺CD8⁺ or CD4⁺ T cells from indicated tissues of (B) naïve control and *let-7bc2*^{LOF} mice or (C) nCB-treated lungs by representative flow plot and MFI quantification (n=5 per group). (D) RORγt expression by MFI quantification in naïve mice *let-7afd*^{LOF} mice thymus, spleen, and lungs (n=3-4 per group), or (E) nCB-ex-posed lungs (n=5 per group). Data are representative of at least three independent experiments displayed as mean±SEM using student's t-test. *p < 0.05, **p < 0.01, ***p <0.001, ****p<0.0001.

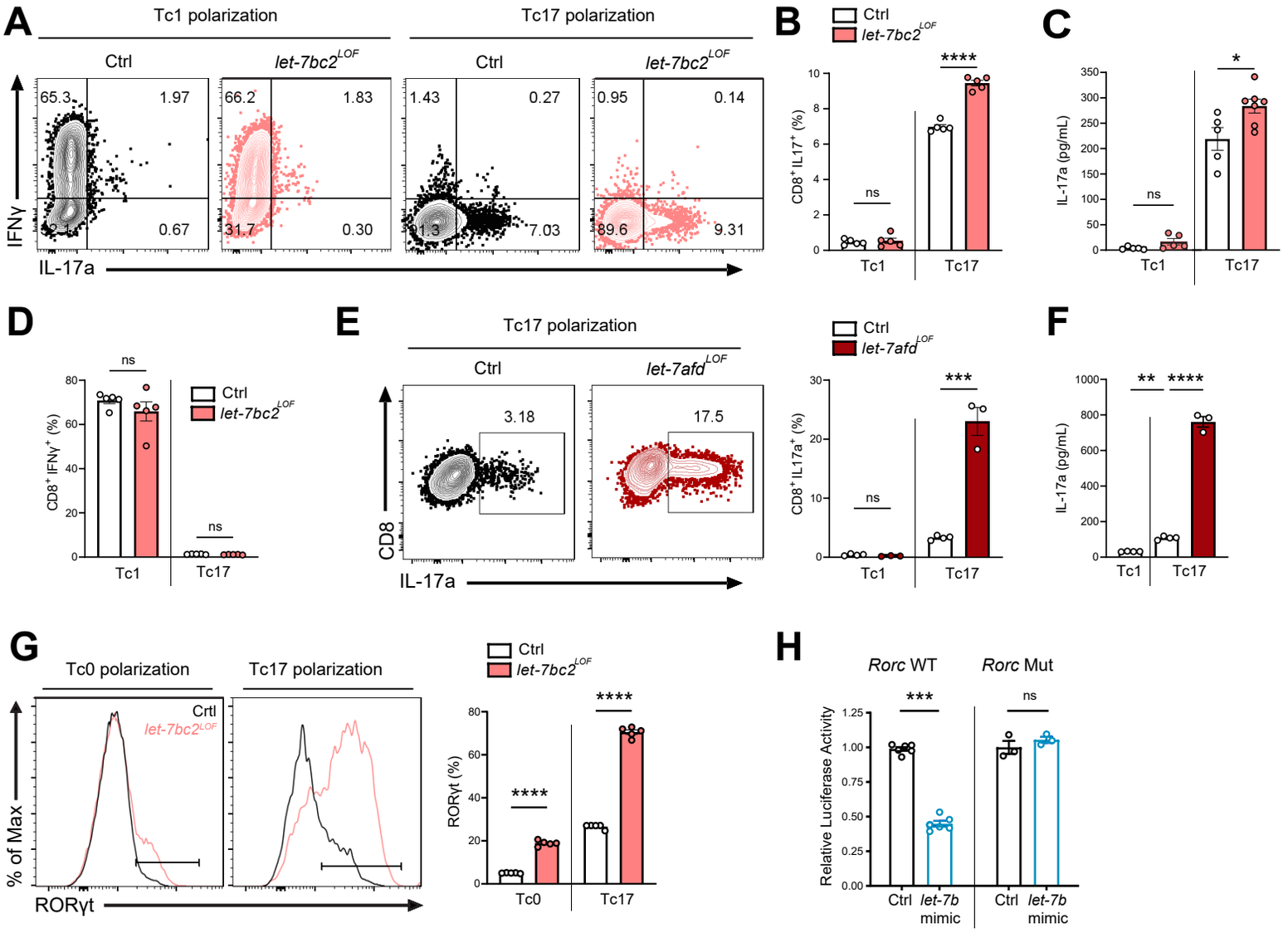

Figure 5. *Let-7* restricts Tc17 *in vitro* differentiation in part via direct targeting of *Rorc* mRNA. (A) Representative flow plots of live TCRβ⁺ CD8⁺, IL-17a⁺ and IFNγ⁺ populations from Tc1 and Tc17 polarized naïve splenic CD8⁺ cells from control and *let-7bc2*^{LOF} mice and (B) quantification of CD8⁺IL-17a⁺ cells (n=5 per group). (C) ELISA of IL-17a from the supernatant of Tc1 and Tc17 polarized control and *let-7bc2*^{LOF} cells (n=5-6 per group). (D) Flow quantification of CD8⁺IFNγ⁺ populations in Tc1 and Tc17 polarized control and *let-7bc2*^{LOF} cells (n=5 per group). (E) Representative flow plots of CD8⁺IL-17a⁺ population frequency in Tc17 polarized cells indicated mice, and (E) quantification of CD8⁺IL-17a⁺ cells from control and *let-7afd*^{LOF} mice polarized under Tc1 or Tc17 conditions. (F) ELISA of IL-17a from control Tc1 (n=4), control Tc17 (n=4), and *let-7afd*^{LOF} Tc17 (n=3) polarized cells. (G) Representative flow plot and quantification of RORγt from Tc0 or Tc17 differentiated naïve splenic CD8⁺ T cells isolated from control and *let-7bc2*^{LOF} mice (n=5 per group). (H) Control (*Rorc* WT) or binding site mutant (*Rorc* Mut) 3' UTRs of *Rorc* were cloned downstream of the renilla luciferase reporter. Plasmids were cotransfected with either a control-miR (black bars) or *let-7b* mimic (blue bars) duplex into cultured cells. Reporter activity was measured 24 hours after transfection and normalized to firefly activity. Data are representative of three independent experiments (A-G) or carried out in triplicate (H) and displayed as mean±SEM using student's t-test. *p < 0.05, **p < 0.01, ***p <0.001, ****p<0.0001.

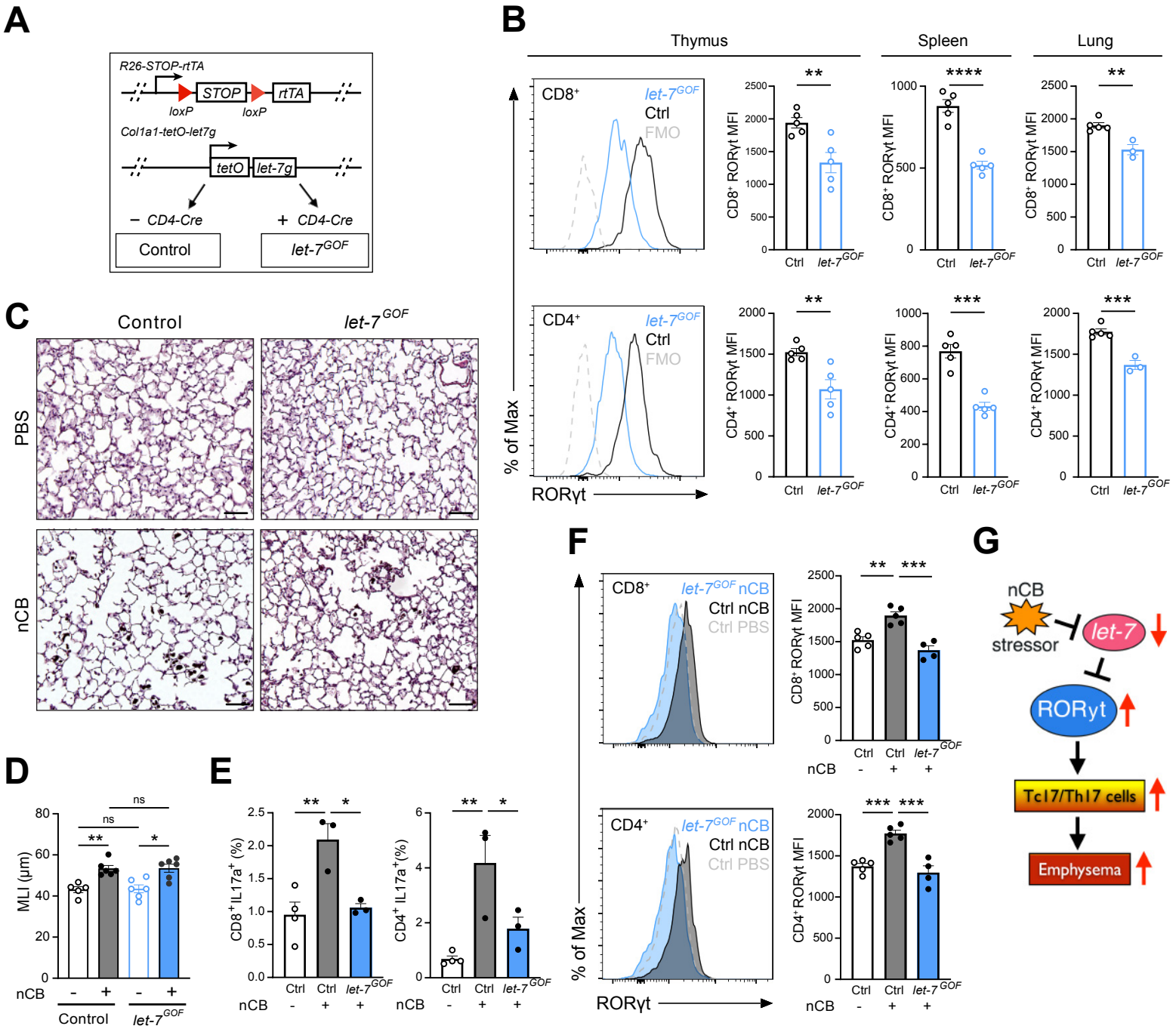

Figure 6. Enforced *let-7* expression in T cells restrains induction of RORγt and Tc17/Th17 inflammation in lungs of nCB-exposed mice. (A) Schematic outlining our T cell-inducible *let-7g* mouse model (*let-7*^{GOF}). (B) Flow analysis of RORγt expression in live, TCRβ$^+$CD8$^+$ or CD4$^+$ T cells from (B) naïve control and *let-7*^{GOF} mice in thymus, spleen, and lungs (n=3-5 per group). (C) Control and *let-7*^{GOF} mice were treated with PBS vehicle or nCB then analyzed. Representative H&E-stained lung sections from PBS- and nCB-exposed mice as indicated on each panel (x20 magnification; scale bars, 50μm) (D) MLI measurements from indicated mice (n=5-6 per group). (E) Flow analysis of lungs gated on live TCRβ$^+$ CD8$^+$ or CD4$^+$ cells for (E) IL-17a$^+$ population frequency (n=3-4 per group) or (F) RORγt expression by representative flow plot and MFI quantification (n=4-5 per group). (G) Figure model for *let-7*/RORγt axis in emphysema pathogenesis. Data are representative of two or three independent experiments and displayed as mean±SEM using student's t-test (B) or two-way ANOVA with Tukey's multiple correction (C,D,E). *p < 0.05, **p < 0.01, ***p <0.001, ****p<0.0001.